THE JOURNAL OF BIOLOGICAL CHEMISTRY VOL. 290, NO. 42, pp. 25745–25755, October 16, 2015
© 2015 by The American Society for Biochemistry and Molecular Biology, Inc. Published in the U.S.A.

Competing Lipid-Protein and Protein-Protein Interactions Determine Clustering and Gating Patterns in the Potassium Channel from *Streptomyces lividans* (KcsA)*

Received for publication, June 4, 2015, and in revised form, August 17, 2015 Published, JBC Papers in Press, September 2, 2015, DOI 10.1074/jbc.M115.669598

M. Luisa Molina[‡1], A. Marcela Giudici[‡1], José A. Poveda[‡2], Gregorio Fernández-Ballester[‡], Estefanía Montoya[‡], M. Lourdes Renart[‡], Asia M. Fernández[‡], José A. Encinar[‡], Gloria Riquelme[§], Andrés Morales[¶], and José M. González-Ros[‡3]

From the [‡]Instituto de Biología Molecular y Celular, Universidad Miguel Hernández, Elche, 03202 Alicante, Spain, the [§]Instituto de Ciencias Biomédicas, Facultad de Medicina, Universidad de Chile, 1027 Santiago, Chile, and the [¶]Departamento de Fisiología, Genética y Microbiología, Universidad de Alicante, 03080 Alicante, Spain

Background: Certain membrane proteins form supramolecular complexes that mediate cooperative cellular functions.
Results: Clustering of KcsA results from competing lipid-protein and protein-protein interactions at nonannular sites and changes its gating.
Conclusion: Clustering effects on gating occur via the Trp^{67}–Glu^{71}–Asp^{80} inactivation triad and its bearing on the selectivity filter.
Significance: These interactions are potential targets for designing ion channel modulators.

There is increasing evidence to support the notion that membrane proteins, instead of being isolated components floating in a fluid lipid environment, can be assembled into supramolecular complexes that take part in a variety of cooperative cellular functions. The interplay between lipid-protein and protein-protein interactions is expected to be a determinant factor in the assembly and dynamics of such membrane complexes. Here we report on a role of anionic phospholipids in determining the extent of clustering of KcsA, a model potassium channel. Assembly/disassembly of channel clusters occurs, at least partly, as a consequence of competing lipid-protein and protein-protein interactions at nonannular lipid binding sites on the channel surface and brings about profound changes in the gating properties of the channel. Our results suggest that these latter effects of anionic lipids are mediated via the Trp^{67}–Glu^{71}–Asp^{80} inactivation triad within the channel structure and its bearing on the selectivity filter.

Since the elucidation of the x-ray structure of KcsA (1–3),[4] this potassium channel from the Gram-positive soil bacterium *Streptomyces lividans* (4) has become an experimental system of choice in many ion channel and membrane protein studies. From the functional view point, the characterization of the KcsA single channel properties has been surrounded by certain controversy. Schrempf and co-workers (4–6), discoverers of KcsA, reported a dependence of channel opening on acidic pH, multiple conductance states with fairly high opening probabilities, and unusual permeabilities to different cations in addition to K^+. In contrast, Miller and co-workers (7, 8), using KcsA reconstituted into planar lipid bilayers, found a single conductance state with a much lower opening probability, as well as orthodox ion selectivity to validate KcsA as a *bona fide* K^+ channel model. Such discrepancies were never fully explained, but still it became accepted that KcsA behaves as a moderately voltage-dependent, K^+-selective channel with low opening probability and the peculiar property of opening in response to intracellular acidic pH. Later on, however, different modes of KcsA activity have been reported, which differ greatly on their opening probability and channel kinetics (9). Moreover, it was found that KcsA may also open at neutral pH when subjected to certain experimental conditions (10). Also, it has been proposed that a more "physiological" version of KcsA might correspond to a supramolecular complex in which the channels would coassemble with polyhydroxybutyrate and inorganic polyphosphates (11), which are reservoir materials in prokaryotes. In our hands, purified KcsA reconstituted into giant liposomes made from asolectin phospholipids exhibits two major patterns of activity in patch-clamp recordings from excised, inside-out membrane patches: (i) a low opening probability (LOP) pattern, seen in ~55% of the recordings, in which channel openings are scarce and result primarily from single channel events or from coupled gating of a few channels, and (ii) a high opening probability (HOP) pattern observed in the remaining 45% of the patches, in which the channels are opened most of the time and exhibit positive cooperativity through

* This work was supported in part by grants from the Spanish Ministerio de Ciencia e Innovación Grants BFU2011-25920 and BFU2012-31359 and Consolider-Ingenio 2010 Grant CSD2-2008-00005. The authors declare that they have no conflicts of interest with the contents of this article.
[1] These authors contributed equally to this work.
[2] Supported by funds from the Ministerio de Ciencia e Innovación José Castillejo Program for short research stays.
[3] To whom correspondence should be addressed. Tel.: 34-96-6658757; Fax: 34-96-6658758; E-mail: gonzalez.ros@umh.es.
[4] The abbreviations used are: KcsA, potassium channel from *S. lividans*; BN, blue native; DDM, dodecyl β-D-maltoside; DOPC, 1,2-dioleoyl-*sn*-glycero-3-phosphocholine; DOPG, 1,2-dioleoyl-*sn*-glycero-3-[phospho-*rac*-(1-glycerol)]; DPPA, 1,2-dipalmitoyl-*sn*-glycero-3-phosphate; HOP, high opening probability; LOP, low opening probability; PA, L-α-phosphatidic acid (egg, chicken); PC, L-α-phosphatidylcholine (egg, chicken); PE, L-α-phosphatidylethanolamine (egg, chicken); PG, L-α-phosphatidylglycerol (egg, chicken); SLB, supported lipid bilayers; Chol, cholesterol.

This is an Open Access article under the CC BY license.

coupled gating of a larger number of channels (12). Because abundant channel clusters were also detected in the giant liposomes, it was speculated that the different functional patterns could arise from "nonclustered" or "clustered" KcsA channels and that the assembly of such supramolecular entities would somehow determine changes in the integrated behavior of the channels involved. Interestingly, KcsA clusters have also been detected *in vivo* both in *S. lividans* and in *Escherichia coli*, suggesting that clusters may be the native form of KcsA in the bacterial membranes (13).

From the structural view point, KcsA is arranged as a homotetramer with subunits of 160 amino acids, each comprising N- and C-terminal cytoplasmic domains and two transmembrane α-helices, TM1 and TM2, connected by a short "pore" helix and a P-loop containing the characteristic TVGYG sequence of the selectivity filter in potassium channels. A further examination of the KcsA crystal structure reveals that it contains noncovalently bound lipid (2, 14) identified as phosphatidylglycerol (PG) (15). Tight binding prevents these lipids from dissociating appreciably from the protein by treatments such as detergent solubilization, and indeed, they cocrystallize with the protein and can be seen in the x-ray structure. The crystallographic evidence and other studies (16) conclude that the PG binding sites in KcsA have the features of the so called "nonannular" sites (17), which usually correspond to clefts or grooves between transmembrane helices or at protein-protein interfaces (18, 19). In particular, nonannular sites in KcsA include a deep cleft on the protein surface, between the pore helix and TM2 of adjacent subunits, which bind *in vitro* other anionic phospholipids, in addition to PG, in a rather unspecific manner (16, 20, 21), and their occupancy seems important for a number of KcsA features. These features include its folding, tetramerization, structural stability, and channel function and therefore make it extremely interesting to study the interactions involved (22–24), which might even be potentially useful targets for the design of ion channel modulators.

Here we report on the role of anionic phospholipids in determining the extent of KcsA clustering, which seemingly occurs as a consequence of competing lipid-protein and protein-protein interactions at the nonannular sites of the channel and brings about changes in the gating properties. In regard to the latter, our results suggest that such changes are mediated via the Trp^{67}–Glu^{71}–Asp^{80} inactivation triad within the channel structure and its bearing on the selectivity filter.

Materials and Methods

Cholesterol (Chol) and asolectin (L-α-phosphatidylcholine from soybean type 2-S) were purchased from Sigma. DOPC, DOPG, PA, PC, PE, and PG, were purchased from Avanti Polar Lipids. Alexa Fluor® 647 C2-maleimide and 3,3′-dioctadecyloxacarbocyanine perchlorate (DiOC18(3)) were from Molecular Probes. DDM was from Calbiochem.

Cloning and Mutagenesis of KcsA—The pT7–837KcsA containing the R64A-KcsA gene mutant was kindly donated by Professor A. Killian (Utrecht University, Utrecht, Holland). The R89A-KcsA mutant was obtained through site-directed mutagenesis, using the wild-type gene inserted into the pQE30 (Qiagen) plasmid as a template. The S22C-KcsA mutant was prepared as described previously (12). All mutations were confirmed by dideoxynucleotide sequencing.

Overexpression and Purification of KcsA—Expression of the wild-type KcsA protein, S22C and R89A mutants were performed in *E. coli* M15 (pRep4) cells, whereas R64A mutant was expressed in *E. coli* strain BL21(λDE3). Purification and determination of protein concentrations were performed as described (25). Yields ranging from 1 to 2 mg of purified, DDM-solubilized, tetrameric KcsA per liter of culture were obtained. The purified protein batches were also analyzed by SDS-PAGE (25).

Blue Native PAGE—Blue native (BN)-PAGE was performed in linear 4–16% (w/v) polyacrylamide gradient gels (26–28). Shortly before starting BN-PAGE, DDM-solubilized KcsA was incubated in the absence or in the presence of increasing concentrations of the corresponding phospholipids as mixed micelles containing 5 mM DDM. Just before their application onto the gel, sample aliquots containing 10 μg of DDM-solubilized protein were mixed with 5% Coomassie Brilliant Blue G stock solution in 750 mM aminocaproic acid and 1 mM SDS to a final 4:1 (by weight) DDM to Coomassie ratio. Electrophoresis was initiated at 85 V for 30 min and then continued at 200 V for 2.5 h, at 4 °C. After electrophoresis, the gels were stained overnight with colloidal Coomassie Blue G 250 (CCB) (29). All gels were scanned and analyzed with ImageQuant TL, version 2005 software (Molecular Dynamics).

Reconstitution of KcsA—Large unilamellar vesicles were prepared from (i) asolectin, (ii) PC:PG:Chol mixtures (both at 50:25:25 and 70:5:25 molar ratios), or (iii) PC:PA:Chol mixtures (both at 50:25:25 and 70:5:25 molar ratios), at 25 mg/ml in 10 mM Hepes, pH 7.5, 100 mM KCl (reconstitution buffer) and stored in liquid N_2 (30). DDM-solubilized wild-type KcsA or mutant proteins were incubated for 30 min with the above vesicles previously resolubilized in 3 mM DDM at a lipid:tetrameric KcsA protein molar ratio of 500:1, and proteoliposomes were formed by detergent removal by gel filtration, as described (12). The reconstituted samples were centrifuged for 30 min at 300,000 × *g*. The pellet was resuspended into reconstitution buffer to a protein concentration of 1 mg/ml, divided into 50-μg aliquots, and stored in liquid N_2 (25).

Electrophysiology—Multilamellar giant liposomes (up to ~100 μm in diameter) were prepared by submitting a mixture of the reconstituted vesicles from above (containing 50 μg of wild-type KcsA or mutants at a lipid to tetrameric protein molar ratio of 500:1) and either asolectin, PC:PA:Chol, or PC:PG:Chol lipid vesicles (25 mg of total lipids), to a cycle of partial dehydration/rehydration (12). Cholesterol was included in the phospholipid mixtures to facilitate giant liposome formation and handling. The resulting giant liposomes have a final lipid:tetrameric protein molar ratio of 46,800:1. Standard, inside-out patch-clamp recordings (31) were carried out on excised patches from the giant liposomes, as reported previously (12). The pipette (extracellular) solution contained 10 mM Hepes buffer, pH 7, 100 mM KCl, and the bath (intracellular) solution contained 10 mM MES buffer, pH 4, 100 mM KCl. Voltage ramps or different holding potentials were routinely imposed on the membrane patches to record channel currents (see details in the figure legends). The extent of rectification of

the *I*/*V* curves was assessed by determining the "rectification index," calculated as the quotient between the whole outward and inward currents recorded during the voltage-ramp protocol.

Supported Lipid Bilayers (SLB) Containing Fluorescently Labeled KcsA—The sulfhydryl-containing mutant KcsA S22C was fluorescently labeled with a maleimide Alexa probe (Alexa Fluor® 647 C2-maleimide; Molecular Probes), as reported (12). Planar bilayers were prepared as described by Chiantia *et al.* (32). Briefly, Alexa-labeled KcsA was reconstituted at 10,000:1, lipid to protein molar ratio in lipid vesicles of the indicated compositions. After a dilution to 0.7 mg/ml of lipid in 10 mM Hepes, pH 7, 100 mM KCl, the sample was bath-sonicated for ~15 min to obtain small unilamellar vesicles. 150 μl of the sample were then placed on a freshly cleaved mica substrate glued to a glass coverslip within an open chamber. To induce vesicle fusion and SLB formation, 3 mM Ca^{2+} was added, rapidly diluted with 400 μl of buffer, and incubated for 15 min at 37 °C. Then the chamber was rinsed thoroughly with prewarmed buffer to remove Ca^{2+} and nonfused vesicles. Control experiments to check for the homogeneity of lipid distribution in the SLBs were done always before measuring KcsA distribution (not shown). To do that, the fluorescent probe 3,3′-dioctadecyloxacarbocyanine perchlorate was incorporated in the liposomes, by its addition to the lipid mixtures when in the chloroform:methanol (2:1) solution used in the initial stages of the liposome formation protocol (30).

Confocal microscopy was performed on an laser scanning microscope Meta 510 system (Carl Zeiss, Jena, Germany) using a 40 × NA 1.2 UV-VIS-IR C Apochromat water immersion objective. SLB samples with Alexa-labeled KcsA were excited with the 633-nm line of a helium-neon laser, and the emitted light was filtered through a 650-nm long pass filter. In control experiments, DiO C18 (3) was excited with the 488-nm line of an argon laser, and the emitted light was filtered through a 505–550-nm band pass filter. Images were processed and analyzed with Scion Image (Scion Corp.).

Molecular Modeling—KcsA-DPPA complexes were built using the KcsA structure having cocrystallized lipids (2) (Protein Data Bank code 1K4C). The partial lipid structures seen in the crystal were used as a scaffold to build the entire DPPA lipid molecule. Lipid-protein contacts were optimized by energy minimization (see below).

Modeling of KcsA in the open conformation was done by homology, using the crystal structure of the open calcium-gated potassium channel MthK as a template (33) (Protein Data Bank code 1LNQ). The sequence alignment was made with CLUSTALW (34) at the European Bioinformatics Institute site and manually supervised (final 24% identity and 40% similarity). The homology modeling was performed in the Swiss-Model protein modeling server (35) at the ExPASy Molecular Biology site under project mode. Structure preparation for modeling was made using DeepView, version 4.1 (36). The model was evaluated using PROCHECK to show the residues in the allowed regions of the Ramachandran plots (37). Model refinements were carried out as described by Molina *et al.* (38), followed by energy minimization. This latter process involved an initial short steepest descent minimization to remove bumps. Next, we performed a simulated annealing minimization in which the simulation cell was slowly cooled toward 0 K by downscaling the atom velocities. The entire system was subject to an equilibration process before the molecular dynamics simulation. The equilibration consisted of an initial minimization of the fixed backbone atoms. Next, the restrained α-carbon atoms were minimized, and a short molecular dynamics (10 ps) minimization was performed to reduce the initial incorrect contacts and to fill the empty cavities. Finally, under periodic boundary conditions in the three coordinate directions, the full system was simulated at 310 K for 0.2 ns. All dynamic simulations were performed using Yasara (39) with the force field AMBER03 (40). The cutoff used for long range interactions was set at 10 Å.

The above open KcsA model was used to predict dimeric KcsA-KcsA interactions. The docking prediction was accomplished with GRAMM-X v.1.2.0 using default conditions. The solutions were checked and filtered manually, discarding those without biological significance, and then evaluated in terms of energy. The final model chosen was that having the highest interaction energy and the lowest van der Waals clashes. Finally, we perform molecular dynamic simulation on the resulting dimeric KcsA, following the protocol stated above.

As an alternative to build a dimer of open KcsA channels, we used the crystal structure of the dimeric potassium transporter TrkH (41) (Protein Data Bank code 3PJZ) as a scaffold to superimpose the three-dimensional structures of two open KcsA channels. The criteria for the superimposition were the correct alignment of the pore filter and the base of the pore helix.

The energy of the models and the docking complexes were tested using FoldX (42, 43) on the CRG site. Molecules were edited and reconstructed with the general purpose molecular modeling software Yasara (39). The final molecular graphic representations were created using PyMOL, version 1.6.

Results

Modeling Lipid-Protein versus Protein-Protein Interactions—Specific interactions of anionic phospholipids with nonannular binding sites at intersubunit crevices in the KcsA homotetramer were first evidenced crystallographically (2) and more recently modeled (21). Fig. 1*A* focuses on the details of such interaction at the level of the extracellular membrane-water interphase and shows that Arg^{89} at one of the KcsA subunits and Arg^{64} at the contiguous subunit forming the intersubunit crevice interact with the phospholipid, "clogging" the crevice's entrance and forcing the side chain of Trp^{67} toward the channel core, where it interacts with Glu^{71} and Asp^{80}. Such Trp^{67}–Glu^{71}–Asp^{80} triad has been reported to play a critical role on the dynamics and conformational stability of the channel selectivity filter and to determine inactivation in KcsA (44), an analogous process to C-type inactivation in eukaryotic K_v channels. The involvement of Arg^{89} and mainly Arg^{64} residues in the interaction with anionic lipids at these nonannular channel sites has been confirmed by NMR experiments (23) and MD simulations (45).

On the other hand, KcsA is known to self-associate into clusters, both *in vivo* and *in vitro* (12, 13, 46, 47). Our hypothesis is that such clusters are responsible for the observed HOP pat-

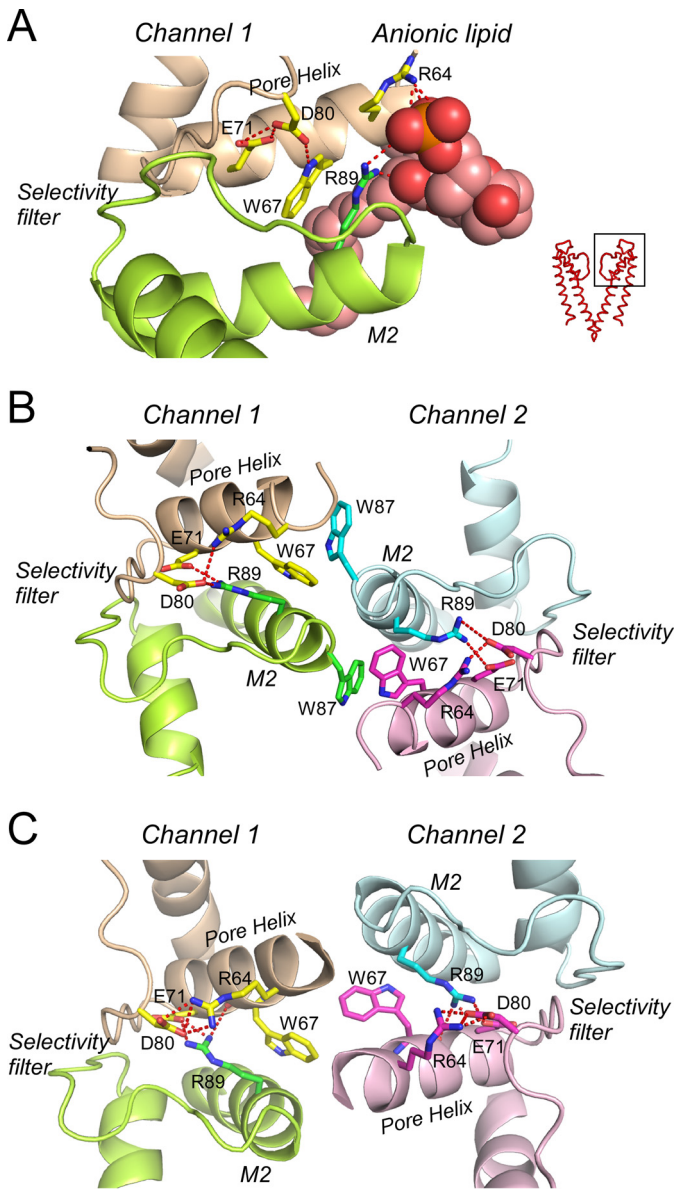

FIGURE 1. **Lipid-protein and protein-protein interactions at nonannular lipid binding sites.** *A* shows a top view (normal to the membrane plane) of an extracellular portion comprising amino acid residues 62–101 (roughly indicated by the *box* on the small diagram to the *right* of *A*) in the crystallographic structure of KcsA (Protein Data Bank code 1K4C) defining one of the four intersubunit crevices acting as nonannular lipid binding sites. A DPPA molecule (atoms represented as *spheres*) has been drawn bound to such a site, using as a scaffold the partial lipid structure appearing in the protein crystal (see "Materials and Methods"). Adjacent protein subunits defining the nonannular site are colored in *light brown* and *green*. The one-letter codes and numbering in the KcsA sequence for the main amino acid residues involved in the interactions have been included. Hydrogen bonds are indicated by *red dashed lines*. It should be noted that the Trp^{67}–Glu^{71}–Asp^{80} inactivation triad is fully configured and that the lipid polar head interacts primarily with Arg^{64} and Arg^{89}. *B* shows the results from computer docking two KcsA channels in an attempt to model a cluster. In this case, the KcsA sequence was previously modeled on the basis of homology onto the open structure of MthK (see "Materials and Methods"). The nonannular binding sites, flanked by the pore helix and M2 in each channel, interact now with the M2 from the adjacent channel (channel 2; subunits colored in *light blue* and *pink*), whereas the inactivation triad has been disrupted. *C* shows the results of modeling the two KcsA channel cluster based on the x-ray structure of the potassium transporter TrkH, which already crystallizes as a dimer (see "Materials and Methods"). Notice that in this case, the nonannular binding site interacts with the pore helix from the adjacent channel, but the effect of such interaction on the disruption of the inactivation triad is identical.

terns of KcsA activity, where the channels are opened most of the time and exhibit coupled gating (12). Therefore, in an attempt to explain how the individual channels could be assembled into clusters to give rise to channel activity with a high opening probability, we performed molecular docking between two adjacent KcsA molecules, using an open channel model of KcsA based on the x-ray open channel structure of MthK as a template (33). The reason for choosing MthK for these studies is that it still remains as the only crystal structure of a potassium channel having open both the inner and outer channel gates, and therefore, it provides the best possible available structure to model the almost permanently open HOP patterns in KcsA. The presence of lipid at the nonannular binding sites prevents docking between the two channels, and therefore, lipids were eliminated from the model. In the absence of the competing lipids (Fig. 1*B*), the intersubunit crevice defining the nonannular sites in each channel becomes now wider (the distance between the α-carbons of Pro^{63} in the pore helix and Trp^{87} in M2 segment increase 1–2 Å, as predicted by the model), being occupied by the N-terminal end of transmembrane M2 from the other channel, which contributes Trp^{87} to the interaction network. As a consequence of docking, the Trp^{67} side chain rotamer pointing away from the channel central core becomes now favored, thus disrupting the interactions within the Trp^{67}–Glu^{71}–Asp^{80} triad. Moreover, Arg^{64} and mainly Arg^{89} interact now with Glu^{71} and Asp^{80}, further contributing to the disassembly of the Trp^{67}–Glu^{71}–Asp^{80} triad responsible for channel inactivation. In other words, the model predicts that a clustered KcsA channel should have different gating and inactivation properties than those seen when anionic phospholipids occupy the nonannular sites of the channel.

As a second approach to test the above hypothesis, we took advantage of the reported x-ray structure of the potassium transporter TrkH (41), which already crystallizes as a dimer and therefore does not require any docking procedure to be applied. These circumstances should make the dimeric TrkH an adequate structure to model potassium channel clusters. In this case, it is the N-terminal end of the pore helix of one channel (instead of the M2, as mentioned above) that goes closer to the also wider intersubunit crevice in the adjacent channel (Fig. 1*C*). Nonetheless, the consequences of such interaction on the Trp^{67}–Glu^{71}–Asp^{80} triad are practically identical to those seen in the docking above, because the positioning of the Trp^{67}, Arg^{64}, and Arg^{89} side chains in the dimer structure contributes similarly to disrupt the interactions within the inactivation triad.

From the above observations, two related predictions can be made: (i) binding of anionic lipids to the nonannular sites should compete with KcsA clustering and (ii) assuming that clustering is indeed a determinant factor of gating behavior, anionic phospholipids should be expected to influence the frequency of appearance of LOP or HOP activity patterns. These two predictions are tested below.

Effects of Lipids on the Assembly/Disassembly of KcsA Clusters—Mixed micelles containing the purified KcsA channel protein solubilized in DDM and different concentrations of specific lipids have been used here to evaluate the extent of KcsA clustering by BN-PAGE, a method of choice to study the

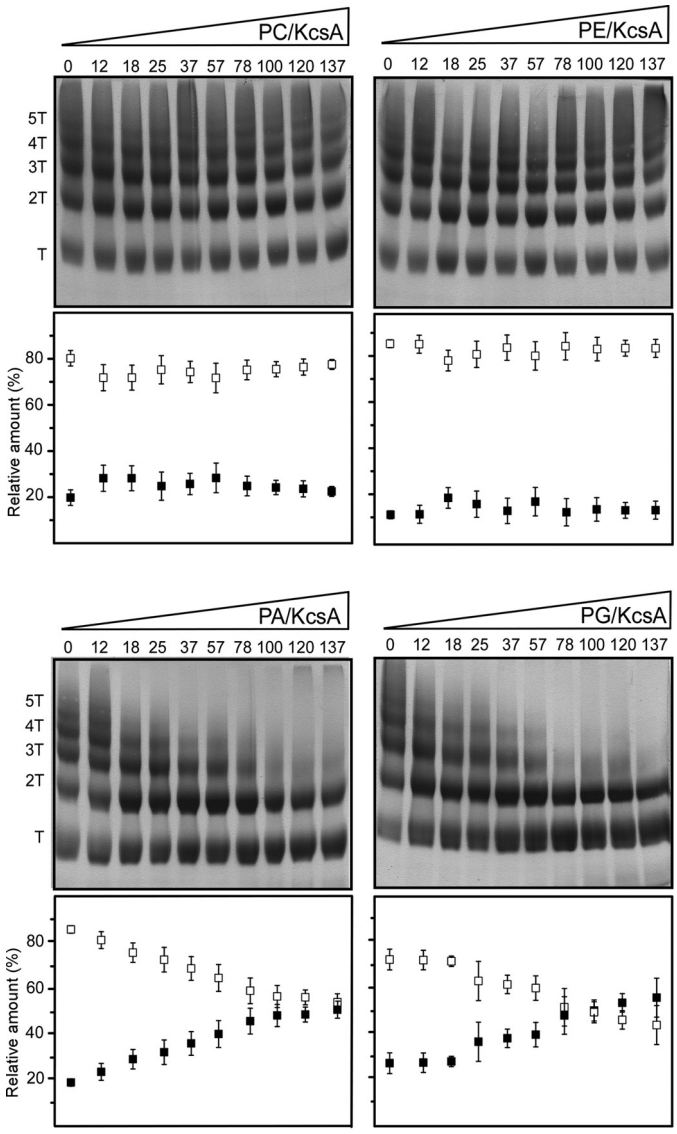

FIGURE 2. **Blue Native PAGE analysis of phospholipid effects on the disassembly of KcsA clusters in mixed micelles.** Mixed micelles containing KcsA and either PC, PE, PG, and PA at the indicated phospholipid to KcsA molar ratios were prepared and analyzed by BN-PAGE. Representative gels for each condition and the results from densitometry are expressed as percentages of T (*closed squares*) and nT (*open squares*) bands relative to the sum of all the bands present within each gel lane are shown. *T* stands for the KcsA tetramer, whereas *nT* refers to the sum of 2T, 3T, 4T, and 5T cluster species having 2, 3, 4, and 5 times the molecular weight of the KcsA tetramer. The values represent the averages ± S.E. of five different gels from each condition.

organization of protein complexes (27, 48–50) including KcsA (26). In BN-PAGE, samples are first solubilized with a mild detergent, usually digitonin or DDM, but it is the negative charge from the Coomassie Brilliant Blue bound to the hydrophobic protein surfaces what determines the electrophoretic mobility. Fig. 2 shows that in the absence of added lipids, the DDM-solubilized protein (*left-hand lane* in all gels) exhibits several bands able to enter the gel, which correspond to different KcsA supramolecular assemblies, which remain as such despite detergent presence (26). The fastest migrating band in the gels is the well known KcsA homotetramer (labeled as *T species* in the figure), whereas the other gel bands correspond to supramolecular clusters comprising 2, 3, 4, and 5 tetrameric channels (labeled *2T*, *3T*, *4T*, and *5T* in the figure). Fig. 2 also shows that increasing the amount of zwitterionic phospholipids (PC or PE in *upper panel*, respectively) in the mixed micelles, regardless of the phospholipid to protein ratio, have no significant effects on the relative abundances of the KcsA species detected by BN-PAGE. Conversely, when anionic phospholipids (PG or PA in *lower panel*) are used in the experiments, disassembly of the larger clusters occurs progressively as the phospholipid to protein ratio is increased, so that eventually the gels show mostly T and 2T KcsA species instead of the more complex starting population of clustered species. Quantitative analysis of cluster disassembly caused by the anionic phospholipids shows no apparent differences between the effects of either PG or PA, suggesting that the concentration-dependent process requires just a negatively charged anionic phospholipid to take place.

In addition to the mixed micelles from above, SLBs have also been used as an experimental system to assess the concentration-dependent effects of anionic phospholipids on KcsA clusters. SLBs are likely to model native membranes better than mixed micelles and also lack detergents, thus providing data complementary to those from above. Fig. 3 shows that fluorescently labeled KcsA in the SLBs indeed forms clusters of variable sizes, up to 1–2 microns in diameter. The abundance of such clusters decreases dramatically, and their size decreases slightly when the presence of anionic lipids in the supported bilayer is increased, thus qualitatively confirming the observation from the mixed micelles above on the ability of high levels of anionic phospholipids to interfere on the assembly of KcsA into clusters.

Effects of Lipids on KcsA Function—We reconstituted KcsA into giant liposomes made from mixtures of different phospholipids to assess their effects on channel function by patch-clamp techniques. Fig. 4 (*A* and *B*) shows that under these conditions the reconstituted KcsA still exhibits both LOP and HOP patterns of channel activity, comparable in all aspects to those described in detail when using asolectin phospholipids for reconstitution of wild-type KcsA (12). However, the frequencies of appearance of such activity patterns are now found to be dependent on the relative proportion of anionic to zwitterionic phospholipids used in the experiments (Fig. 4*C*). Thus, giant liposomes containing only 5% of either PA or PG in a PC/cholesterol matrix have a high percentage of patches exhibiting HOP patterns of activity (~70% of the recordings, taking together the two populations of PA- and PG-containing giant liposomes; $n = 84$). Conversely, giant liposomes containing 25% of either PA or PG in the lipid matrix show an increased presence of LOP patterns, *i.e.* a marked decrease in the frequency of appearance of HOP patterns (which account for only ~30% of the recordings; $n = 91$; $p < 0.01$ when compared against the group of 5% anionic lipids, *z* test). Interestingly, the frequency of appearance of HOP patterns reported in asolectin lipids (12), which is between those found in the lipid media containing 5 or 25% anionic phospholipids from above (Fig. 4*C*), seems consistent with the report that asolectin lipids contain 10–13% anionic phospholipids (51). These observations indicate that the ability of KcsA to exhibit HOP patterns of channel activity is inversely related to the concentration of ani-

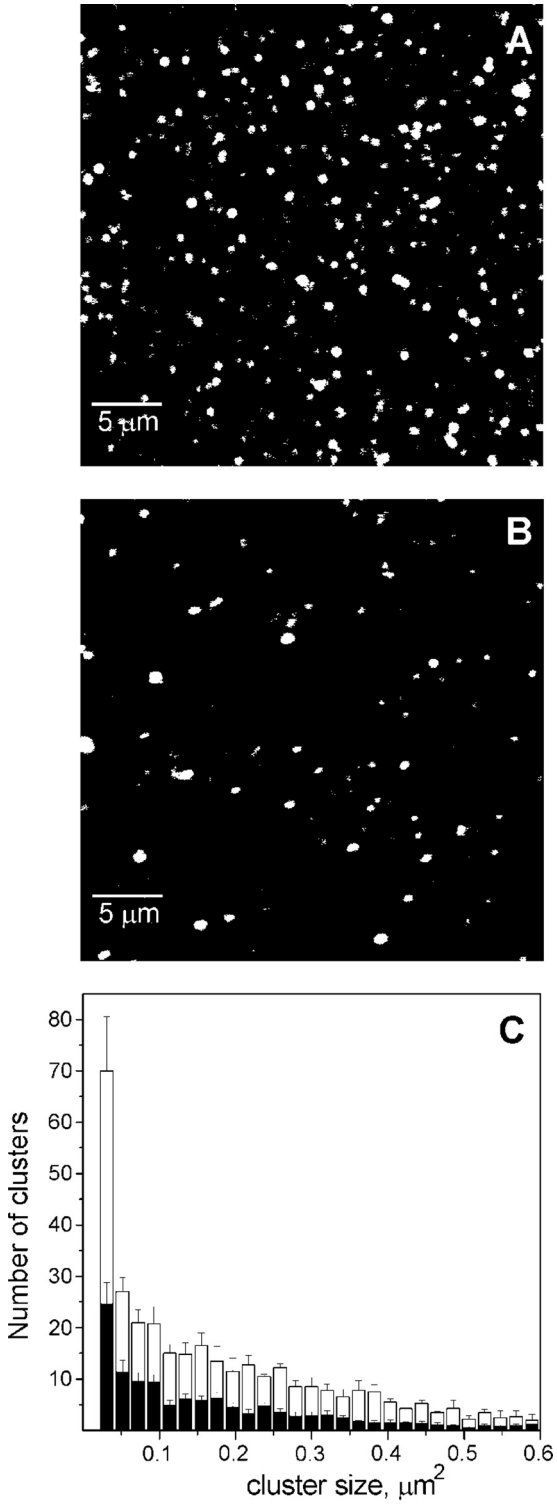

FIGURE 3. **KcsA clusters in supported bilayers.** Representative fluorescence microscopy images of a confocal cross-section (parallel to the bilayer plane) of SLBs containing Alexa 647-labeled KcsA. *A*, SLBs made from a DOPC:DOPG mixture at a 95:5 molar ratio. *B*, SLBs of pure DOPG. Large and highly fluorescent array-like protein complexes of variable sizes are seen in both cases. *C*, size distribution of KcsA clusters in the two SLBs samples from above. *Bars* represent the number of clusters observed per image in the pure DOPG (*filled*) and in the DOPC:DOPG (*open*) samples. The values are the averages ± S.E. of four to nine images from each of three different SLB samples prepared in each condition.

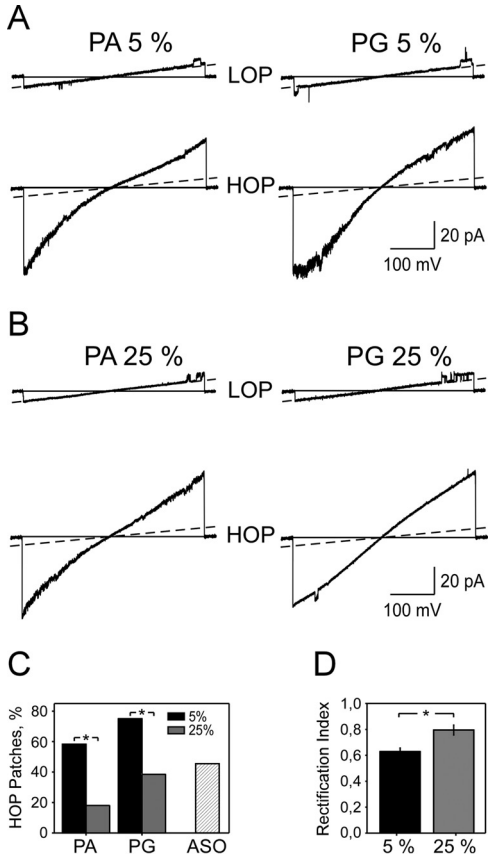

FIGURE 4. **Effects of anionic phospholipids on the gating patterns of KcsA reconstituted into giant liposomes.** *A* and *B* show representative voltage ramps (−200 to 200 mV from a 0 mV holding potential, 133 mV/s) showing typical LOP and HOP activity patterns of KcsA obtained by patch clamping excised, inside-out patches from giant liposomes containing KcsA reconstituted into 5 or 25% of anionic lipid (PA or PG; see "Materials and Methods"). In this figure, as well as in Fig. 6, *dashed lines* indicate the closed channel states, and *thin continuous lines* indicate zero current level. Channel openings appear as upward (at positive voltages) or downward (at negative voltages) deflections over the closed state line. *C* shows the percentage of patches showing HOP patterns in each of the above groups. Giant liposomes containing only 5% (*black columns*) of either PA or PG in the PC/cholesterol matrix showed 58.3% ($n = 14$ from 24 patches) or 75.0% ($n = 45$ from 60 patches) of patches exhibiting HOP patterns of activity, respectively, whereas giant liposomes containing 25% (*gray columns*) of either PA or PG in the lipid matrix show 17.9% ($n = 7$ from 39 patches) or 38.5% ($n = 20$ from 52 patches) HOP patterns of activity, respectively. To compare the occurrence of a characteristic of interest between two groups, we used the *z* test. *Asterisks* indicate significant differences ($p < 0.05$) in the occurrence of HOP pattern activity in samples containing different proportions of the same anionic lipid. The effect of anionic lipids on HOP activity occurrence was even more evident when comparing together the data of PA and PG for the two concentrations tested (see "Results" for details). The *right-hand column* in *C*, labeled *ASO*, indicates the percentage of HOP patterns found when reconstituting KcsA into giant liposomes made from asolectin lipids (45.7%; $n = 75$ from 164 patches). *D*, column histogram of the rectification index (see "Materials and Methods") of the HOP pattern of KcsA channels reconstituted in 5 and 25% anionic lipids.

onic phospholipids within the reconstituted membrane bilayer. In any case, it should be noted that at comparable concentrations, PA was always more efficient than PG in decreasing the percentage of HOP patterns.

The presence of anionic phospholipids in the lipid matrix has an additional effect on the observed HOP currents: although the samples containing 5% anionic lipids, in which HOP patterns are predominant, show a clear inward rectification at negative potentials (rectification index: 0.63 ± 0.03, $n = 59$; see Fig. 4, *lower traces* (HOP) in *A* and the *black column* in *D*), those

containing 25% anionic lipids show HOP currents with a lesser inward rectification (rectification index: 0.79 ± 0.04, $n = 27$; $p < 0.01$; see Fig. 4, *lower traces* (HOP) *B* and the *gray column* in *D*). Such different features were previously observed as variants of HOP patterns upon reconstitution of KcsA in asolectin lipids (12).

Analysis of KcsA Single Mutants—In the previous paragraphs, we hypothesized that the different patterns of channel clustering and gating observed in the presence of increasing concentrations of anionic phospholipids could be explained on the basis of differential interactions involving key amino acid residues, namely Arg^{64}, Arg^{89}, and Trp^{67}, that bear on the integrity of the Trp^{67}–Glu^{71}–Asp^{80} inactivation triad and thus on the properties of the selectivity filter. Therefore, we conducted experiments with several mutants of KcsA to test our hypothesis.

The electrostatic interaction between anionic phospholipids and positively charged amino acid residues in the KcsA sequence is believed to constitute the basis for lipid binding to the nonannular sites (16, 20). Therefore, substitution of the Arg^{64} or Arg^{89} residues by uncharged amino acids in KcsA mutants should disfavor the stabilization of anionic phospholipids at such sites, and according to our working hypothesis, such mutants should be expected to display an altered pattern of channel clustering and gating. Fig. 5 shows that compared with the wild-type channel in Fig. 2, the R64A KcsA mutant is indeed relatively insensitive to the effect of anionic phospholipids on the disassembly of channel clusters observed by BN-PAGE. Conversely, the R89A mutant still shows a partial response of cluster disassembly by anionic phospholipids, more markedly to PA than to PG, suggesting that lipid interaction and the subsequent cluster disassembly relates mainly to the presence of the Arg^{64} residue in the channel sequence.

As to the functional responses, the two arginine mutant channels have in common a marked loss of their ability to inactivate. Fig. 6 (*A* and *B*) shows that the predominant pattern seen in the R64A mutant is very similar to the HOP pattern exhibited by the wild-type channel (68%; 17 of 25 patches), including the characteristic coupled gating observed in channel openings and closings within the HOP recordings. Single channel recordings taken from this mutant channel (Fig. 6*C*) show that the channel conductance is also similar to that reported for the wild-type channel (12), but the channel opening probability is greatly increased, as expected, approaching that reported by others for this and other mutant channels such as the E71A mutant (52), considered an archetypical "noninactivating" channel. As different from the above, the R89A channel mutant shows unusual HOP patterns (73%; 30 of 41 patches), with lower overall current levels throughout the voltage ramps, particularly at negative potentials (Fig. 6*D*), and a marked loss of the coupled gating feature (Fig. 6*E*), as if the ensemble of channels within the clusters were now opening and closing in a mostly independent manner. We termed this behavior of the R89A mutant as an "uncoupled" HOP pattern, which is similar to that reported by Perozo and co-workers (52) for several KcsA mutant channels. Nonetheless, the R89A mutant has in common with the R64A mutant a similar conductance and channel opening probability in single channel recordings (Fig. 6*F*).

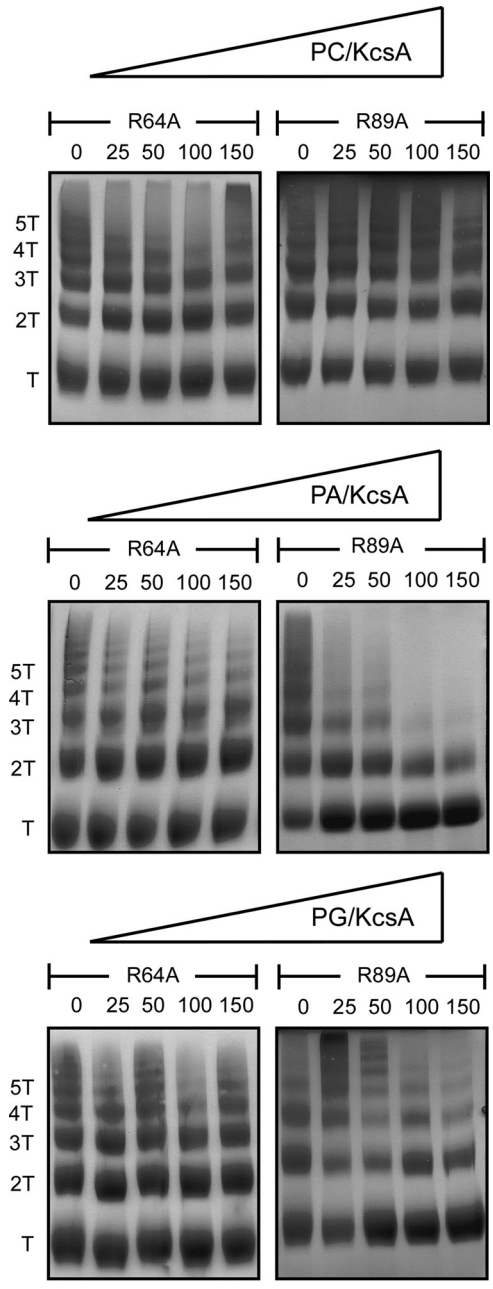

FIGURE 5. **Blue Native PAGE analysis of the effects of phospholipids on the disassembly of clusters of KcsA arginine mutants in mixed micelles.** Mixed micelles containing the indicated KcsA arginine mutants and either PC (*top row*), PA (*middle row*), or PG (*bottom row*), at the indicated phospholipid to KcsA molar ratios, were analyzed by BN-PAGE. Experimental conditions and details within the figure are as in Fig. 2.

Despite having been reported by others (44, 52), W67F and E71A KcsA mutants were also prepared in our lab to compare their behavior under our experimental conditions with the arginine mutants from above. In agreement with such reports, we found that, even more markedly than in the R89A mutant, HOP recordings in both the E71A and W67F mutants have an even lower extent of channel coupling, *i.e.* were also uncoupled HOPs, and when recorded as single channels, exhibited also a high P_o, as expected from these two amino acid residues being part of the Trp^{67}–Glu^{71}–Asp^{80} inactivation triad (data no shown).

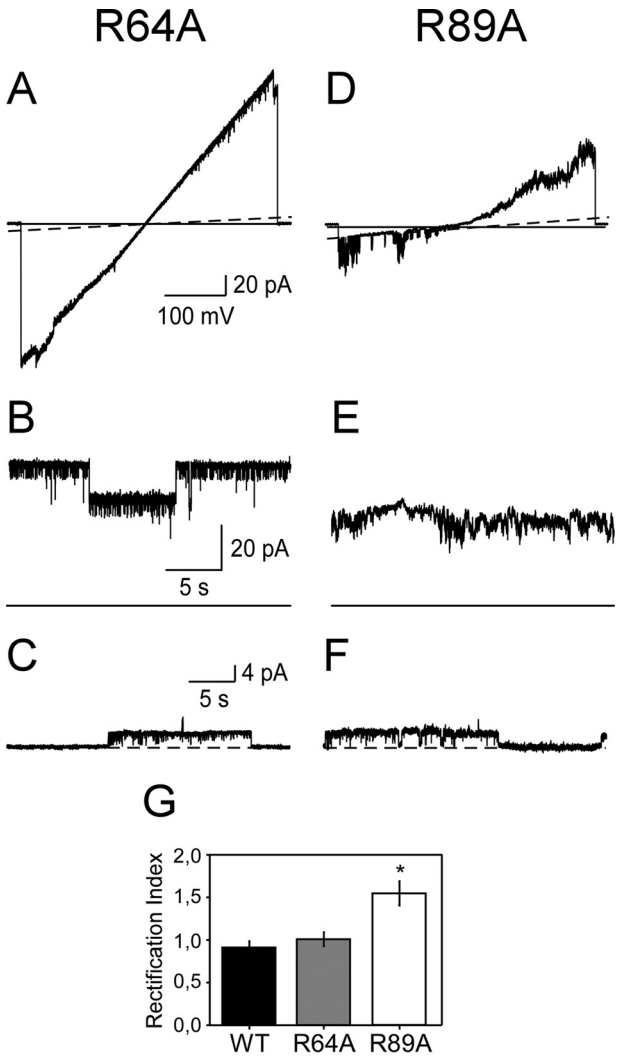

FIGURE 6. **Gating patterns observed in R64A and R89A KcsA mutants.** *A* and *D* show representative voltage ramps illustrating the predominant activity patterns of the R64A (*A*; 17 of 25 patches, 68% of the cases) and the R89A (*D*; 30 of 41 patches, 73% of the cases) KcsA mutants, respectively, reconstituted into giant liposomes made from asolectin lipids. Experimental conditions and drawing details are as in Fig. 4. Notice that the R64A mutant shows HOP patterns of activity very similar to those seen in wild-type KcsA (12) and exhibits coupled gating, as illustrated in the continuous recording taken at +150 mV shown in *B*. None of these features are clearly present in the R89A mutant (*D* and *E*), which exhibits mainly uncoupled HOPs (see "Results"). *C* and *F* show single channel recordings taken also at +150 mV of the two mutant channels to illustrate that despite the above differences; the channel conductance and opening probability when analyzed at the single channel level are similar in both cases. *G* shows a column histogram of the rectification index of the HOP pattern of the wild-type KcsA, as well as those of the R64A and R89A mutant channels.

Finally, it should be noted that the uncoupled HOPs seen in the R89A mutant, as well as those in the W67A and E71A mutants (not shown), showed *I*/*V* curves with outward rectification (rectification index for R89A mutant: 1.54 ± 0.12, n = 30; see Fig. 6*G*), instead of the inward rectification or almost ohmic behavior seen in conventional HOP patterns from either the wild-type KcsA or the R64A mutant (rectification index: 0.92 ± 0.06, n = 25, and 1.01 ± 0.08, n = 17, for wild-type and R64A mutant channels, respectively; see Fig. 6*G*). Outward rectification is a hallmark feature of KcsA single channels (5, 8, 12), thus further supporting that the uncoupled HOP recordings arise from channels that, despite forming clusters, act independently.

Discussion

Channel activity in KcsA results from a concerted equilibrium between two defined ion gates within the protein structure (53). The inner gate is formed by the intracellular transmembrane helix bundle crossing, which is destabilized at acidic pH, shifting the equilibrium toward its open conformation. On the other hand, the outer gate at the selectivity filter defines primarily the channel opening probability and may shift its conformation equilibrium from the permeation state toward a nonpermeation state, causing channel inactivation. Both the conformational state and functional responses of KcsA seem strongly modulated by its surrounding membrane milieu (43, 54–56), probably through an alteration of one or both gating equilibria. So far, different mechanisms have been proposed to explain such effects. On one hand, although still controversial, nonspecific electrostatic interactions between anionic lipids and the N-terminal portion of the protein are proposed to favor the open conformation of the inner gate of the channel (57), resulting in increased activity. On the other hand, specific interactions of anionic lipids with the nonannular binding sites of KcsA have been proposed to modulate ion channel function through its influence on the outer gate (45, 56), although there is not a clear explanation for such an effect. In this work, we propose that a competition between lipid-protein and protein-protein interactions at the nonannular binding sites constitutes a central element in such KcsA modulation.

Both *in vivo* (13) and *in vitro* (12, 25, 46, 47), KcsA assembles into supramolecular clusters, which could even be the predominant forms in which this channel is present in bacterial membranes (12, 25). Here we report that both in a mixed lipid/detergent micellar system and in supported bilayers, the presence of anionic phospholipids modulates assembly/disassembly of such KcsA clusters. Therefore, low proportions of anionic phospholipids allow KcsA to remain associated into clusters, whereas higher concentrations lead to cluster disassembly. Moreover, such conditions of high or low proportion of anionic phospholipids in reconstituted giant liposomes containing KcsA increase the frequency of appearance of either LOP or the more complex HOP patterns of channel activity, respectively, in patch clamp recordings. Thus, the effects of the anionic phospholipids on the assembly/disassembly of clusters and on the appearance of HOP/LOP patterns of activity are correlative and suggest that the more complex HOP recordings indeed arise from large channel clusters, whereas LOP recordings originate mostly from nonclustered, phospholipid-bound KcsA channels. It should be noted here that experimental variables such as the presence of detergent, lipids, or the lipid to protein ratios used in reconstitution greatly influence KcsA assembly, and therefore, the comparison of results from the different experimental approaches used here should only be done in qualitative terms.

In an attempt to find a cause and effect relationship for the above phenomena, we modeled the consequences of the interaction of either an anionic phospholipid or another tetrameric channel at the nonannular site of KcsA. Fortunately, these

interactions are partly documented from x-ray crystallographic data of both the anionic phospholipid-KcsA complex (2) and that of the dimeric potassium transporter TrkH (40), thus providing a valuable experimental support to our models. Opposite to the channel-channel interaction, binding of the phospholipid to the nonannular site on the channel allows Trp^{67} to form the Trp^{67}–Glu^{71}–Asp^{80} triad, which should leave the phospholipid-bound channel prone to inactivate. Because KcsA is a homotetramer, there are four identical nonannular sites, each of them acting on just one of the four rows of Thr^{75}-Val^{76}-Gly^{77}-Tyr^{78}-Gly^{79} residues from each subunit, which contribute their carbonyl groups to configure the selectivity filter. It is to be expected that anionic lipids disrupt channel-channel interactions at more than one of such sites to affect sufficiently the selectivity filter conformation as to make inactivation a truly effective process, whose occurrence should be dependent on the phospholipid concentration. Obviously, a readily inactivating channel should produce recordings characterized by a low channel opening probability, *i.e.* a LOP pattern of activity, as has been found experimentally.

On the contrary, because the inactivation triad in clustered KcsA is predictably disrupted because channel-channel interaction causes that Trp^{67} swings away from its Glu^{71} and Asp^{80} partners, these clustered channels would not be expected to inactivate as readily as the phospholipid-bound, nonclustered KcsA channel does. This is indeed the case in the observed HOP patterns of channel activity.

Finally, site-directed mutagenesis at specific residues involved in the interaction with the anionic phospholipids was carried out to provide additional evidence to support or to discard our working hypothesis. In this regard, Arg^{64} and Arg^{89} residues are claimed to be responsible for electrostatic interaction with the anionic phospholipids at the nonannular protein sites and their substitution by alanine should be expected to minimize such interactions, partly preventing cluster disassembly and channel inactivation. This seems clearly the case in the R64A mutant, which does not disassemble significantly when in presence of anionic phospholipids, as shown by the BN-PAGE assay, and exhibits an essentially noninactivating pattern of channel activity, very similar to the HOP patterns in wild-type KcsA, in which coupled-gated currents are observed throughout. These results further evidence of a major role for Arg^{64} in lipid interaction.

Conversely, the R89A mutant shows clusters that partly disassemble in response to the presence of anionic phospholipids, more markedly to PA than to PG, and exhibits lower current levels and less coupled gating than the wild-type KcsA. The larger effect of PA over PG on cluster disassembly could be due to the fact that, in the appropriate environment, PA could become a dianionic species, which may further favor the interaction with the positively charged groups in the protein. Indeed, PA has been reported to have a higher affinity than PG to bind to the nonannular sites of KcsA (21). As to the decrease in the current level observed in the R89A mutant, we found that both the single channel conductance and the opening probability in these two arginine mutants were similar, and therefore, the lower current levels observed in the R89A mutant should be mainly attributed to a diminished capacity to recruit individual

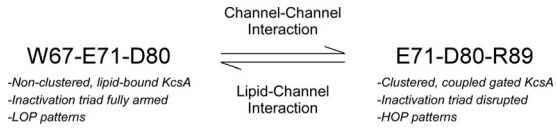

SCHEME 1

channels into the coupled-gated clusters. Therefore, the behavior of the R89A mutant channel suggests that the Arg^{89} residue is important to maintain gating features characteristic of HOP patterns in wild-type KcsA, because its absence results in uncoupled HOP patterns with an outward rectification. This is also similarly observed in the W67F and E71A mutants, and therefore, it seems that the residues involved in determining channel inactivation, including Arg^{89}, are also involved in conferring channel coupling and current rectification properties through a still undefined mechanism.

The above experimental observations, as well as the predictions from the models, are depicted in a simplified manner in Scheme 1. Interaction with the anionic phospholipid, in which Arg^{64} is heavily involved, impedes cluster assembly and leaves Trp^{67}, Glu^{71}, and Asp^{80} residues free to form the inactivation triad, resulting in individual, lipid-bound channels (LOP patterns of channel activity). On the contrary, cluster assembly displaces Trp^{67} from the inactivation triad. Such a displacement seems difficult to reverse because the remaining inactivation triad members (Glu^{71} and Asp^{80}) are now predictably stabilized by interaction with Arg^{89}, which swings into the channel core as a consequence of channel-channel interaction. This results in clustered channels quite unable to inactivate, which may exhibit either (i) coupled gating, as in the conventional HOP patterns characteristic of wild-type KcsA, or (ii) uncoupled HOPs, when in the absence of strategic amino acid residues, as seen in some of the mutants above. Interestingly, altering interactions among residues equivalent to those configuring the inactivation triad in KcsA have been found to change selectivity, block, and current rectification properties in a Kir channel (58).

KcsA clusters have been detected *in vivo* (13), and indeed, they might account for the complex patterns of electrical activity reported earlier for this channel (4, 5). Nonetheless, the assembly of clusters *in vitro* upon membrane reconstitution from purified channel preparations is a protein concentration-dependent phenomenon (12), and therefore, the experimental conditions used in reconstitution by the different authors, particularly the lipid to protein ratios used, which ranges within more than an order of magnitude, should be expected to greatly influence the occurrence of clustering and its functional consequences. For instance, clustering might go unnoticed under conditions such as those used to obtain recordings in planar lipid membranes, which use a very low concentration of KcsA, sometimes in the presence of detergents or organic solvents, which may also compete for binding to the KcsA nonannular sites. Indeed, the low opening probability mode of KcsA is believed to be predominant in planar bilayer experiments (9). In any case, considering that the molar ratio of KcsA to phospholipids in our giant liposome samples ranged approximately from 1:10,000 to 1:46,800, it becomes obvious that the affinity of KcsA to associate with other KcsA channels to form clusters

above a certain threshold of protein concentration is much higher than that to bind the anionic phospholipids contained in the bilayer, and therefore, cluster formation should be favored under our experimental conditions.

All the evidence from above seemingly completes an scenario in agreement with the starting hypothesis, in which competing lipid-protein or protein-protein interactions at the nonannular sites of KcsA determine both the occurrence of clustering and changes in gating behavior. The latter changes seemingly result from interfering with the assembly of the Trp^{67}–Glu^{71}–Asp^{80} inactivation triad, which in turn bears on the conformation of the selectivity filter. In other words, clustered KcsA channels have different dynamics and conformational stability at the selectivity filter than nonclustered, phospholipid-bound KcsA. Both clustering- and lipid-related effects in gating behavior have also been reported for other channels (59–64), and although diverse mechanistic explanations have been given, it may be possible that phenomena similar to that reported here might also underline some of those observations.

Author Contributions—J. M. G.-R. conceived and coordinated the study and wrote the paper. M. L. M. conceived the study and designed, performed, and analyzed the experiments shown in Figs. 4 and 6. A. M. G. designed, performed, and analyzed the experiments shown in Figs. 2 and 5. J. A. P. designed, performed, and analyzed the experiments shown in Fig. 3. G. F.-B. performed and analyzed the models shown in Fig. 1. E. M. performed some of the experiments shown in Fig. 6. E. M., M. L. R., A. M. F., A. M., J. A. E., and G. R. provides discussion and critical revision of the manuscript. A. M. performed also the statistical analysis. G. R. also kindly lent his laboratory for the electrophysiology experiments shown in Fig. 4. All authors approved the final version of the manuscript.

Acknowledgments—We thank Dr. Petra Schwille for allowing Dr. Poveda the use of laboratory facilities at the Biotechnologischees Zentrum (BIOTEC), Technische Universität Dresden. We also thank Dr. Salvatore Chiantia and Dr. Jakob Schweizer for help with SLB experiments, Dr. Erica Kremer and Dr. Antoinette Killian for the pT7–837KcsA containing the R64A-KcsA gene mutant, and Dr. Antonio V. Ferrer-Montiel for critical reading of the manuscript. Eva Martínez provided excellent technical assistance throughout.

References

1. Doyle, D. A., Morais Cabral, J., Pfuetzner, R. A., Kuo, A., Gulbis, J. M., Cohen, S. L., Chait, B. T., and MacKinnon, R. (1998) The structure of the potassium channel: molecular basis of K+ conduction and selectivity. *Science* **280,** 69–77
2. Zhou, Y., Morais-Cabral, J. H., Kaufman, A., and MacKinnon, R. (2001) Chemistry of ion coordination and hydration revealed by a K^+ channel-Fab complex at 2.0 A resolution. *Nature* **414,** 43–48
3. Uysal, S., Vásquez, V., Tereshko, V., Esaki, K., Fellouse, F. A., Sidhu, S. S., Koide, S., Perozo, E., and Kossiakoff, A. (2009) Crystal structure of full-length KcsA in its closed conformation. *Proc. Natl. Acad. Sci. U.S.A.* **106,** 6644–6649
4. Schrempf, H., Schmidt, O., Kümmerlen, R., Hinnah, S., Müller, D., Betzler, M., Steinkamp, T., and Wagner, R. (1995) A prokaryotic potassium ion channel with two predicted transmembrane segments from *Streptomyces lividans*. *EMBO J.* **14,** 5170–5178
5. Meuser, D., Splitt, H., Wagner, R., and Schrempf, H. (1999) Exploring the open pore of the potassium channel from *Streptomyces lividans*. *FEBS Lett.* **462,** 447–452
6. Splitt, H., Meuser, D., Borovok, I., Betzler, M., and Schrempf, H. (2000) Pore mutations affecting tetrameric assembly and functioning of the potassium channel KcsA from *Streptomyces lividans*. *FEBS Lett.* **472,** 83–87
7. Heginbotham, L., Kolmakova-Partensky, L., and Miller, C. (1998) Functional reconstitution of a prokaryotic K^+ channel. *J. Gen. Physiol* **111,** 741–749
8. LeMasurier, M., Heginbotham, L., and Miller, C. (2001) KcsA: it's a potassium channel. *J. Gen. Physiol* **118,** 303–314
9. Chakrapani, S., Cordero-Morales, J. F., and Perozo, E. (2007) A quantitative description of KcsA gating II: single-channel currents. *J. Gen. Physiol* **130,** 479–496
10. Zakharian, E., and Reusch, R. N. (2004) *Streptomyces lividans* potassium channel KcsA is regulated by the potassium electrochemical gradient. *Biochem. Biophys. Res. Commun.* **316,** 429–436
11. Zakharian, E., and Reusch, R. N. (2004) Functional evidence for a supramolecular structure for the *Streptomyces lividans* potassium channel KcsA. *Biochem. Biophys. Res. Commun.* **322,** 1059–1065
12. Molina, M. L., Barrera, F. N., Fernández, A. M., Poveda, J. A., Renart, M. L., Encinar, J. A., Riquelme, G., and González-Ros, J. M. (2006) Clustering and coupled gating modulate the activity in KcsA, a potassium channel model. *J. Biol. Chem.* **281,** 18837–18848
13. Hegermann, J., Overbeck, J., and Schrempf, H. (2006) *In vivo* monitoring of the potassium channel KcsA in *Streptomyces lividans* hyphae using immuno-electron microscopy and energy-filtering transmission electron microscopy. *Microbiology* **152,** 2831–2841
14. Valiyaveetil, F. I., Zhou, Y., and MacKinnon, R. (2002) Lipids in the structure, folding, and function of the KcsA K^+ channel. *Biochemistry* **41,** 10771–10777
15. Demmers, J. A., van Dalen, A., de Kruijff B., Heck, A. J., and Killian, J. A. (2003) Interaction of the K+ channel KcsA with membrane phospholipids as studied by ESI mass spectrometry. *FEBS Lett.* **541,** 28–32
16. Deol, S. S., Domene, C., Bond, P. J., and Sansom, M. S. (2006) Anionic phospholipid interactions with the potassium channel KcsA: simulation studies. *Biophys. J.* **90,** 822–830
17. Lee, A. G. (2004) How lipids affect the activities of integral membrane proteins. *Biochim. Biophys. Acta* **1666,** 62–87
18. Cheng, M. H., Xu, Y., and Tang, P. (2009) Anionic lipid and cholesterol interactions with $\alpha 4\beta 2$ nAChR: insights from MD simulations. *J. Phys. Chem. B* **113,** 6964–6970
19. Fersht, A. R. (1999) *Structure and Mechanism in Protein Science: A Guide to Enzyme Catalysis and Protein Folding*, 3rd Ed., W. H. Freeman and Company, New York
20. Marius, P., Alvis, S. J., East, J. M., and Lee, A. G. (2005) The interfacial lipid binding site on the potassium channel KcsA is specific for anionic phospholipids. *Biophys. J.* **89,** 4081–4089
21. Triano, I., Barrera, F. N., Renart, M. L., Molina, M. L., Fernández-Ballester, G., Poveda, J. A., Fernández, A. M., Encinar, J. A., Ferrer-Montiel, A. V., Otzen, D., and González-Ros, J. M. (2010) Occupancy of nonannular lipid binding sites on KcsA greatly increases the stability of the tetrameric protein. *Biochemistry* **49,** 5397–5404
22. Barrera, F. N., Renart, M. L., Poveda, J. A., de Kruijff, B., Killian, J. A., and González-Ros, J. M. (2008) Protein self-assembly and lipid binding in the folding of the potassium channel KcsA. *Biochemistry* **47,** 2123–2133
23. Marius, P., de Planque, M. R., and Williamson, P. T. (2012) Probing the interaction of lipids with the non-annular binding sites of the potassium channel KcsA by magic-angle spinning NMR. *Biochim. Biophys. Acta* **1818,** 90–96
24. van Dalen, A., Hegger, S., Killian, J. A., and de Kruijff, B. (2002) Influence of lipids on membrane assembly and stability of the potassium channel KcsA. *FEBS Lett.* **525,** 33–38
25. Molina, M. L., Encinar, J. A., Barrera, F. N., Fernández-Ballester, G., Riquelme, G., and González-Ros, J. M. (2004) Influence of C-terminal protein domains and protein-lipid interactions on tetramerization and stability of the potassium channel KcsA. *Biochemistry* **43,** 14924–14931
26. Giudici, A. M., Molina, M. L., Ayala, J. L., Montoya, E., Renart, M. L., Fernández, A. M., Encinar, J. A., Ferrer-Montiel, A. V., Poveda, J. A., and González-Ros, J. M. (2013) Detergent-labile, supramolecular assemblies of KcsA: relative abundance and interactions involved. *Biochim. Biophys.*

Acta **1828,** 193–200
27. Schägger, H., and von Jagow, G. (1991) Blue native electrophoresis for isolation of membrane protein complexes in enzymatically active form. *Anal. Biochem.* **199,** 223–231
28. Schägger, H., Cramer, W. A., and von Jagow, G. (1994) Analysis of molecular masses and oligomeric states of protein complexes by blue native electrophoresis and isolation of membrane protein complexes by two-dimensional native electrophoresis. *Anal. Biochem.* **217,** 220–230
29. Neuhoff, V., Stamm, R., and Eibl, H. (1985) Clear background and highly sensitive protein staining with Coomassie Blue dyes in polyacrylamide gels: a systematic analysis. *Electrophoresis* **6,** 427–448
30. Riquelme, G., Lopez, E., Garcia-Segura, L. M., Ferragut, J. A., and Gonzalez-Ros, J. M. (1990) Giant liposomes: a model system in which to obtain patch-clamp recordings of ionic channels. *Biochemistry* **29,** 11215–11222
31. Hamill, O. P., Huguenard, J. R., and Prince, D. A. (1991) Patch-clamp studies of voltage-gated currents in identified neurons of the rat cerebral cortex. *Cereb. Cortex* **1,** 48–61
32. Chiantia, S., Kahya, N., and Schwille, P. (2005) Dehydration damage of domain-exhibiting supported bilayers: an AFM study on the protective effects of disaccharides and other stabilizing substances. *Langmuir* **21,** 6317–6323
33. Jiang, Y., Lee, A., Chen, J., Cadene, M., Chait, B. T., and MacKinnon, R. (2002) Crystal structure and mechanism of a calcium-gated potassium channel. *Nature* **417,** 515–522
34. Thompson, J. D., Higgins, D. G., and Gibson, T. J. (1994) CLUSTAL W: improving the sensitivity of progressive multiple sequence alignment through sequence weighting, position-specific gap penalties and weight matrix choice. *Nucleic Acids Res.* **22,** 4673–4680
35. Schwede, T., Kopp, J., Guex, N., and Peitsch, M. C. (2003) SWISS-MODEL: An automated protein homology-modeling server. *Nucleic Acids Res.* **31,** 3381–3385
36. Guex, N., and Peitsch, M. C. (1997) SWISS-MODEL and the Swiss-Pdb-Viewer: an environment for comparative protein modeling. *Electrophoresis* **18,** 2714–2723
37. Laskowski, R. A., Rullmannn, J. A., MacArthur, M. W., Kaptein, R., and Thornton, J. M. (1996) AQUA and PROCHECK-NMR: programs for checking the quality of protein structures solved by NMR. *J. Biomol. NMR* **8,** 477–486
38. Molina, M. L., Barrera, F. N., Encinar, J. A., Renart, M. L., Fernández, A. M., Poveda, J. A., Santoro, J., Bruix, M., Gavilanes, F., Fernández-Ballester, G., Neira, J. L., and González-Ros, J. M. (2008) N-type inactivation of the potassium channel KcsA by the Shaker B "ball" peptide: mapping the inactivating peptide-binding epitope. *J. Biol. Chem.* **283,** 18076–18085
39. Krieger, E., Koraimann, G., and Vriend, G. (2002) Increasing the precision of comparative models with YASARA NOVA: a self-parameterizing force field. *Proteins* **47,** 393–402
40. Duan, Y., Wu, C., Chowdhury, S., Lee, M. C., Xiong, G., Zhang, W., Yang, R., Cieplak, P., Luo, R., Lee, T., Caldwell, J., Wang, J., and Kollman, P. (2003) A point-charge force field for molecular mechanics simulations of proteins based on condensed-phase quantum mechanical calculations. *J. Comput. Chem.* **24,** 1999–2012
41. Cao, Y., Jin, X., Huang, H., Derebe, M. G., Levin, E. J., Kabaleeswaran, V., Pan, Y., Punta, M., Love, J., Weng, J., Quick, M., Ye, S., Kloss, B., Bruni, R., Martinez-Hackert, E., Hendrickson, W. A., Rost, B., Javitch, J. A., Rajashankar, K. R., Jiang, Y., and Zhou, M. (2011) Crystal structure of a potassium ion transporter, TrkH. *Nature* **471,** 336–340
42. Guerois, R., Nielsen, J. E., and Serrano, L. (2002) Predicting changes in the stability of proteins and protein complexes: a study of more than 1000 mutations. *J. Mol. Biol.* **320,** 369–387
43. Schymkowitz, J., Borg, J., Stricher, F., Nys, R., Rousseau, F., and Serrano, L. (2005) The FoldX web server: an online force field. *Nucleic Acids Res.* **33,** W382–W388
44. Cordero-Morales, J. F., Jogini, V., Chakrapani, S., and Perozo, E. (2011) A multipoint hydrogen-bond network underlying KcsA C-type inactivation. *Biophys. J.* **100,** 2387–2393
45. Weingarth, M., Prokofyev, A., van der Cruijsen, E. A., Nand, D., Bonvin, A. M., Pongs, O., and Baldus, M. (2013) Structural determinants of specific lipid binding to potassium channels. *J. Am. Chem. Soc.* **135,** 3983–3988
46. Raja, M., and Vales, E. (2009) Effects of sodium chloride on membrane fusion and on the formation of aggregates of potassium channel KcsA in *Escherichia coli* membrane. *Biophys. Chem.* **142,** 46–54
47. Seeger, H. M., Bortolotti, C. A., Alessandrini, A., and Facci, P. (2009) Phase-transition-induced protein redistribution in lipid bilayers. *J. Phys. Chem. B* **113,** 16654–16659
48. Heuberger, E. H., Veenhoff, L. M., Duurkens, R. H., Friesen, R. H., and Poolman, B. (2002) Oligomeric state of membrane transport proteins analyzed with blue native electrophoresis and analytical ultracentrifugation. *J. Mol. Biol.* **317,** 591–600
49. Nicke, A., Rettinger, J., Mutschler, E., and Schmalzing, G. (1999) Blue native PAGE as a useful method for the analysis of the assembly of distinct combinations of nicotinic acetylcholine receptor subunits. *J. Recept. Signal. Transduct. Res.* **19,** 493–507
50. Vinothkumar, K. R., Raunser, S., Jung, H., and Kühlbrandt, W. (2006) Oligomeric structure of the carnitine transporter CaiT from *Escherichia coli*. *J. Biol. Chem.* **281,** 4795–4801
51. McCormick, J. I., and Johnstone, R. M. (1988) Volume enlargement and recovery of Na^+-dependent amino acid transport in proteoliposomes derived from Ehrlich ascites cell membranes. *J. Biol. Chem.* **263,** 8111–8119
52. Cordero-Morales, J. F., Cuello, L. G., Zhao, Y., Jogini, V., Cortes, D. M., Roux, B., and Perozo, E. (2006) Molecular determinants of gating at the potassium-channel selectivity filter. *Nat. Struct. Mol. Biol.* **13,** 311–318
53. Blunck, R., Cordero-Morales, J. F., Cuello, L. G., Perozo, E., and Bezanilla, F. (2006) Detection of the opening of the bundle crossing in KcsA with fluorescence lifetime spectroscopy reveals the existence of two gates for ion conduction. *J. Gen. Physiol* **128,** 569–581
54. Heginbotham, L., LeMasurier, M., Kolmakova-Partensky, L., and Miller, C. (1999) Single *Streptomyces lividans* K^+ channels: functional asymmetries and sidedness of proton activation. *J. Gen. Physiol* **114,** 551–560
55. Imai, S., Osawa, M., Mita, K., Toyonaga, S., Machiyama, A., Ueda, T., Takeuchi, K., Oiki, S., and Shimada, I. (2012) Functional equilibrium of the KcsA structure revealed by NMR. *J. Biol. Chem.* **287,** 39634–39641
56. Marius, P., Zagnoni, M., Sandison, M. E., East, J. M., Morgan, H., and Lee, A. G. (2008) Binding of anionic lipids to at least three nonannular sites on the potassium channel KcsA is required for channel opening. *Biophys. J.* **94,** 1689–1698
57. Iwamoto, M., and Oiki, S. (2013) Amphipathic antenna of an inward rectifier K^+ channel responds to changes in the inner membrane leaflet. *Proc. Natl. Acad. Sci. U.S.A.* **110,** 749–754
58. Dibb, K. M., Rose, T., Makary, S. Y., Claydon, T. W., Enkvetchakul, D., Leach, R., Nichols, C. G., and Boyett, M. R. (2003) Molecular basis of ion selectivity, block, and rectification of the inward rectifier Kir3.1/Kir3.4 K^+ channel. *J. Biol. Chem.* **278,** 49537–49548
59. Undrovinas, A. I., Fleidervish, I. A., and Makielski, J. C. (1992) Inward sodium current at resting potentials in single cardiac myocytes induced by the ischemic metabolite lysophosphatidylcholine. *Circ. Res.* **71,** 1231–1241
60. Goforth, R. L., Chi, A. K., Greathouse, D. V., Providence, L. L., Koeppe, R. E., 2nd, and Andersen, O. S. (2003) Hydrophobic coupling of lipid bilayer energetics to channel function. *J. Gen. Physiol* **121,** 477–493
61. Botelho, A. V., Huber, T., Sakmar, T. P., and Brown, M. F. (2006) Curvature and hydrophobic forces drive oligomerization and modulate activity of rhodopsin in membranes. *Biophys. J.* **91,** 4464–4477
62. Grage, S. L., Keleshian, A. M., Turdzeladze, T., Battle, A. R., Tay, W. C., May, R. P., Holt, S. A., Contera, S. A., Haertlein, M., Moulin, M., Pal, P., Rohde, P. R., Forsyth, V. T., Watts, A., Huang, K. C., Ulrich, A. S., and Martinac, B. (2011) Bilayer-mediated clustering and functional interaction of MscL channels. *Biophys. J.* **100,** 1252–1260
63. Spira, F., Mueller, N. S., Beck, G., von Olshausen, P., Beig, J., and Wedlich-Söldner, R. (2012) Patchwork organization of the yeast plasma membrane into numerous coexisting domains. *Nat. Cell Biol.* **14,** 640–648
64. Mueller, N. S., Wedlich-Söldner, R., and Spira, F. (2012) From mosaic to patchwork: matching lipids and proteins in membrane organization. *Mol. Membr. Biol.* **29,** 186–196